Hindawi
Scientific Programming
Volume 2021, Article ID 4327596, 9 pages
https://doi.org/10.1155/2021/4327596

*Research Article*

# Global Joint Entropy Algorithm-Based Evaluation of Dexmedetomidine Combined Local Anesthetics in Brachial Plexus Block from Ultrasound Images

**Xiujuan Ge**,[1] **Xiaopeng Song**,[2] **and Linyan Li**[3]

[1]*Department of Anesthesia, Jiaozhou Central Hospital of Qingdao, Qingdao 266300, China*
[2]*Department of Anesthesia, Traditional Chinese Medical Hospital of Huangdao District, Qingdao 266300, China*
[3]*Department of Anesthesia, Affiliated Hospital of Weifang Medical College, Weifang, Shandong 261031, China*

Correspondence should be addressed to Linyan Li; fylly1230@wfmc.edu.cn

Received 11 September 2021; Revised 22 October 2021; Accepted 25 October 2021; Published 16 November 2021

Academic Editor: M Pallikonda Rajasekaran



This paper aimed to explore dexmedetomidine combined local anesthetics in brachial plexus block through ultrasound imaging (UI) under global joint entropy algorithm. Patients who underwent upper limb surgery and brachial plexus block were selected as research objects. Patients in group A were given 0.375% ropivacaine and normal saline, and patients in group B were given 0.375% ropivacaine and 1.0 $\mu$g/kg dexmedetomidine. The results of UI were analyzed by global joint entropy-based K-means clustering (GKC) algorithm, and the use effects of the two methods were compared in combination with other postanesthesia manifestations. The results were as follows. The segmentation accuracy (96.21% and 83.52%) of GKC was higher than 82.21% and 70.52% of the local joint entropy-based K-means clustering (LKC) ($P < 0.05$). The duration of sensory and motor block (352.78 ± 45.89 min and 324.38 ± 41.29 min) in group B was significantly longer than 292.28 ± 35.69 min and 256.58 ± 42.76 min in group A ($P < 0.05$). Compared with 84.91 ± 8.77 beats/min and 89.58 ± 7.62 beats/min in group A, mean arterial pressure (70.24 ± 9.77 beats/min and 69.89 ± 8.97 beats/min) in group B was lower at T1 and T2 ($P < 0.05$). The duration of postoperative pain (582.70 ± 51.89 min) in group B was longer than 372.89 ± 49.89 min in group A ($P < 0.05$). The postoperative pain score (2.98 ± 1.08) in group B was significantly lower than 4.48 ± 2.19 in group A ($P < 0.05$). Therefore, dexmedetomidine combined local anesthetics could prolong the duration of sensory and motor nerve block. Besides, dexmedetomidine had sedative and analgesic effects, so as to prolong postoperative pain time and reduce pain degree of patients.

## 1. Introduction

Brachial plexus block is a commonly applied method of anesthesia in upper limb surgery. It is an anesthetic method in which local anesthetics are injected around the brachial plexus nerve trunk to produce nerve conduction block in the area [1]. Brachial plexus block can generally be blocked by the intermuscular groove approach between the anterior and middle scalene muscles. Besides, it can also be blocked by the supraclavicular or the axillary approaches. In addition to these three approaches, there are other 3 approaches to be chosen, such as the subclavian approach, the approach next to coracoid process, and the cervical nerve root approach [2]. The patient should be kept conscious during the surgery. When the patient will feel pain that is caused by the generated stretch during the surgery, analgesia should be conducted.

Dexmedetomidine is a highly selective $\alpha$-2 adrenergic receptor agonist with sedative, anti-inflammatory, hypnotic, and analgesic effects [3]. Ropivacaine is an anesthetic commonly applied in regional anesthesia [4]. El-Boghdadly et al. [5] investigated the mechanism of brachial plexus block and found that intravenous infusion of dexmedetomidine can prolong the time of ropivacaine block. However, there are few domestic research studies on the therapeutic effects of dexmedetomidine combined local anesthetics in the surgery of brachial plexus block.

With the rapid development of computer image processing technology, the application of UI in medical imaging

has gradually become widespread [6]. It is one of the critical tools for clinical pathological diagnosis in medicine. Through the localization and recognition of ultrasonic images and the extraction of graphic features, the pathology is analyzed so that the efficiency of clinical diagnosis is improved. The ultrasonic images for image segmentation of lesions have always been a hot topic in current research [7]. Nallam et al. [8] proposed the LKC, which had a good segmentation effect on images with non-Gaussian noise. The operation process of this algorithm is more complicated, so the segmentation time is relatively long. Based on the above, GKC was put forward in this study, which had a good segmentation effect on ultrasonic images. In recent years, the development of UI has reduced the difficulty of brachial plexus block, thereby promoting the therapeutic effect of nerve block. The brachial plexus block intuitively guided by ultrasonic images is highly effective compared with the traditional brachial plexus block method that only applies the body surface positioning [9].

The GKC and LKC were used for ultrasonic images of 80 patients undergoing brachial plexus block anesthesia, and a comparison of the effects of the two algorithms was conducted. Thus, the diagnostic value of medetomidine combined with ropivacaine was comprehensively evaluated in brachial plexus block.

## 2. Materials and Methods

*2.1. Selection of Research Objects.* In this study, 80 patients were selected as the research objects, who received the upper extremity surgeries with brachial plexus block from November 18, 2019, to May 20, 2020. Based on a random number table method, they were enrolled into groups A and B (40 cases in each group). The grading of American Association of Anesthesiologists (ASA) included the 3 grades (I, II, and III). Patients from group A were given 0.375% ropivacaine and normal saline, while patients from group B were injected with 0.375% ropivacaine and 1.0 $\mu$g/kg dexmedetomidine. Furthermore, the time was controlled within 10 minutes. This experiment had been authorized by the Medical Ethics Committee of the hospital, and the patients and their family members had understood the situation of this experiment and signed the informed consent forms.

The criteria for inclusion were defined to include patients who were treated with the upper extremity surgeries, had the surgery time less than 4 hours, had normal coagulation function, were younger than 45 years old, and had clear consciousness in order to normally take part in this experiment.

The criteria for exclusion were defined to include patients who were allergic to local anesthetics, suffered from infection at the block site, had abnormal heart, liver, and kidney functions, and withdrew from this experiment due to their own reasons.

*2.2. Physical Condition Grading Standards and Observation Indicators.* According to the ASA, the physical conditions of patients could be classified into grade I (patients were normal and healthy), grade II (patients suffered from mild systemic diseases), grade III (patients had severe systemic diseases), grade IV (patients had severe systemic disease and their lives were in danger), grade V (patients were near death with a low surgical success rate), and grade VI (patients suffered from brain death).

Observation indicators were as follows. The heart rate (times/min) and mean arterial pressure (mmHg) of patients from the two groups were recorded at each time point, including before the anesthesia (T0), the surgical duration of 30 minutes (T1), and the end of surgery (T2). When the heart rate exceeded 100 beats/min, anesthesia had to be stopped and esmolol was injected intravenously at 1 mg/kg. When the heart rate was lower than 50 beats/min, atropine was given at 0.3 mg/time. Sensory block evaluation was to score the pain degree of the action sites of the ulnar, median, and musculocutaneous nerves. The total score was 3 points, namely, 0 point for no pain; 1 point for no pain but reaction; and 2 points for pain. The onset time of sensory block was defined as the time from the end of brachial plexus block injection to the time the sensory block of patient with pain (2 points) in the corresponding area of nerve control. Furthermore, the onset time of motor block was presented as the time from the end of brachial plexus block injection until the motor ability with 2 points of the corresponding area controlled by the nerve.

*2.3. Anesthesia Process of Brachial Plexus Block.* The patients from the two groups needed to fast for 10 hours and not to drink for 6 hours before the surgery. Moreover, they should not take any medicine before the surgery. When a patient entered the laboratory, a monitor had to be connected to detect the mean arterial pressure, pulse oxygen saturation, and heart rate of patient in real time. During anesthesia, the patient took a supine position, with the head tilted to one side, the affected upper limbs were placed at 90 degrees to the body, and the hands should be placed on the head. The whole body was in a salute shape, so that the axilla was completely exposed for subsequent puncture operation.

In this study, two experienced physicians performed brachial plexus blocks on patients. GEV730 and Philips U22 Doppler ultrasound diagnostic instrument were used. The probe frequency was 3.5–5.0 MHz. Then, the UI characteristics should be carefully observed at the site of brachial plexus block. The probe was put into the axillary artery of patient to capture a clear image. Besides, the site to be punctured should be sterilized. The puncture needle was set on one side of the probe, and there was a puncture at the interface perpendicular to the brachial plexus nerve. The puncture depth of this needle was observed through the ultrasonic image, so as to reach the designated position and inject the corresponding medicine. Patients from group A received 0.375% ropivacaine and normal saline while patients from group B were administered with 0.375% ropivacaine and dexmedetomidine at 1.0 $\mu$g/kg, and the time was both controlled within 10 minutes.

*2.4. K-Means Clustering Algorithm Based on Global Joint Entropy.* The definition of joint entropy is as follows. The two random variables $A$ and $B$ satisfied the following equation:

$$W_\theta(A,B) = C[L_\theta(A-B)]. \tag{1}$$

In practice, another mathematical expression was often employed to represent the joint entropy, as shown in the following equation:

$$W^{\wedge}_{M,}\theta(A,B) = \frac{1}{M}\sum_{i=1}^{M} L_\theta(a_i - b_i), \tag{2}$$

where $M$ represented the number of all data and $a_i$ and $b_i$ stood for random variables. The energy function equation of GKC was as follows:

$$C_{\mathrm{GCK}}(\Omega_1,\Omega_2) = \min\left\{-\sum_{i=1}^{M}\left(\pi(i,1)\theta^2 h\left(\left\|J_i-\Omega_1\right\|_2\right)+\pi(i,2)\theta^2 h\left(\left\|J_i-\Omega_2\right\|_2\right)\right)+\xi|E|\right\}, \tag{3}$$

where $h(x) = \exp(-x^2/2\theta^2)$ was the Gaussian kernel function and $q$ expressed the width of the kernel. Moreover, $\pi(i,1) = 1 - G(\varphi_i)$ and $\pi(i,2) = 1 - G(\varphi_i)$. Then, the objective function of GKC was calculated by transforming the level set theory and iterative weighting algorithm, as shown in the following:

$$C_{\mathrm{GCK}}(\varphi,\Omega_1,\Omega_2) = \min_{\varphi,\Omega_1,\Omega_2}\left\{-\sum_{i=1}^{M}\theta^2\left(G_h(\varphi_i)\times h\left(\left\|J_i-\Omega_1\right\|_2\right)+(1-G_h(\varphi_i))h\left(\left\|J_i-\Omega_2\right\|_2\right)\right)+\xi\sum_{i=1}^{M}\left|\nabla G_\lambda(\varphi_i)\right|\right\}, \tag{4}$$

where the first item stood for the external energy item, the second item represented the edge length constraint item, the third item meant the symbol distance equation, and $x$ expressed the non-negative parameter item. The zero level set of the level set $j$ was represented by the target contour $E$. Furthermore, the Heaviside function was expressed as $G(\cdot)$, as shown in the following equation:

$$G_\lambda(x) = \frac{1}{2}\left[1+\frac{2}{\pi}\arctan\left(\frac{x}{\lambda}\right)\right]. \tag{5}$$

The derivative equation could be expressed as follows:

$$\begin{aligned}\psi_\lambda(x) &= G'_\lambda(x)\\ &= \frac{\lambda}{\pi\left(\lambda^2+x^2\right)},\end{aligned} \tag{6}$$

where $\lambda = 1$. Since equation (4) was a non-linear function, an iterative weighting algorithm was applied, and the calculation equation was as follows:

$$\theta^2 h\left(\left\|J_i-\Omega_1\right\|_2\right) = -\eta^s_{i,1}\left\|J_i-\Omega_1\right\|_2^2, \tag{7}$$

$$\theta^2 h\left(\left\|J_i-\Omega_2\right\|_2\right) = -\eta^s_{i,2}\left\|J_i-\Omega_2\right\|_2^2. \tag{8}$$

Equations (7) and (8) could meet $-\eta^s_{i,1} = h(\|J_i - \Omega_1^{s-1}\|_2)$ and $-\eta^s_{i,2} = h(\|J_i - \Omega_2^{s-1}\|_2)$.

$\Omega_1^{s-1}$ and $\Omega_2^{s-1}$ stood for the cluster centers, and $-\eta^s_{i,1}$ and $-\eta^s_{i,2}$ represented the weights from the pixel $i$ to the two cluster centers in turn. According to equations (4)–(8), the objective function of the GKC in the $s$-th iteration could be obtained as follows:

$$C_{\mathrm{GCK}}(\varphi,\Omega_1,\Omega_2) = \min_{\varphi,\Omega_1,\Omega_2}\sum_{i=1}^{M}\left\{G_h(\varphi_i)\times\eta^s_{i,1}\left\|J_i-\Omega_1\right\|_2^2+(1-G_h(\varphi_i))\eta^s_{i,2}\left\|J_i-\Omega_2\right\|_2^2+\xi\sum_{i=1}^{M}\left|\nabla G_\varepsilon(\varphi_i)\right|\right\}. \tag{9}$$

The target contour of $j$ was calculated by the standard gradient descent method, which was obtained through the following two steps. Thus, the equations of first step were as follows:

$$\Omega_1^s = \frac{\sum_{i=1}^{M} G_h\left(\varphi_i^{s-1}\right)\eta_{i,1}^s J_i}{\sum_{i=1}^{M} G_h\left(\varphi_i^{s-1}\right)\eta_{i,1}^s}, \tag{10}$$

$$\Omega_2^s = \frac{\sum_{i=1}^{M} G_h\left(1 - G_\lambda\left(\varphi_i^{s-1}\right)\right)\eta_{i,1}^s J_i}{\sum_{i=1}^{M}\left(1 - G_\lambda\left(\varphi_i^{s-1}\right)\right)\eta_{i,2}^s}, \tag{11}$$

where $\Omega_1^s$ and $\Omega_2^s$ stood for the weighted mean values of all pixels in the evolution curve. As for images with uniform gray levels, there was a good segmentation effect. The gradient flow equation was employed to calculate the level set function, and the equation of second step could be shown in the following.

$$\varphi_i^s = \varphi_i^{s-1} - \alpha \frac{\mathrm{d}C_{\mathrm{GCK}}\left(\varphi, \Omega_1, \Omega_2\right)}{\mathrm{d}\varphi_i}, \tag{12}$$

where $\alpha$ represented the step length, which was generally taken as $\alpha = 0.1$, and it also satisfied the following equation:

$$\frac{\mathrm{d}C_{\mathrm{GCK}}\left(\varphi, \Omega_1, \Omega_2\right)}{\mathrm{d}\varphi_i} = G_h\left(\varphi_i\right) \times \left(\eta_{i,1}^s \left\|J_i - \Omega_1\right\|_2^2 - \eta_{i,2}^s \left\|J_i - \Omega_2\right\|_2^2\right) - \xi\psi_\lambda\left(\varphi_i\right)\mathrm{div}\left(\frac{\varphi_i}{\left|\varphi_i\right|}\right). \tag{13}$$

Based on the above steps, the flowchart of GKC in this study was as follows (Figure 1).

*2.5. Simulation Experiment Design.* When verifying the segmentation results of the GKC model, including images without noise (platform 1) and images with salt and pepper noise (platform 2), the GKC model was compared with the LKC model.

For the accuracy of the segmentation results of the GKC model, the Jaccard similarity ratio was used for quantitative analysis, and the equation could be expressed as follows:

$$J\left(\mathrm{DIV}_1, \mathrm{DIV}_2\right) = \frac{\left|\mathrm{DIV}_1 \cap \mathrm{DIV}_2\right|}{\left|\mathrm{DIV}_1 \cup \mathrm{DIV}_2\right|}, \tag{14}$$

where $\mathrm{DIV}_1$ and $\mathrm{DIV}_2$ represented the standard segmentation result and the GKC segmentation result of this study.

*2.6. Statistical Methods.* The data processing of this study was analyzed by SPSS20.0 statistical software. The measurement data were expressed as mean ± standard deviation, which conformed to the normal distribution. There were statistics on the average height, the surgical duration, the time of using the tourniquet, and the brachial plexus block time, block onset time, and block duration of patients from the two groups. In addition, the non-conformity count data were represented by percentage (%), and the Jaccard similarity ratio of the two algorithms was calculated. $P < 0.05$ meant that the difference was statistically substantial.

## 3. Results

*3.1. Comparison of Diagnostic Performance of the Two Algorithms.* In order to compare the effects of GKC and LKC, they were adopted in the ultrasonic images of 80 patients with brachial plexus block anesthesia, and the effects of GKC were significantly better than those of LKC ($P < 0.05$). Figure 2 shows the comparison results of Jaccard similarity ratios of the two algorithms. It was found that the accuracy rate of the GCK model in this study was 96.21% when platform 1 image was segmented, and the accuracy rate of platform 2 was 83.52%. Therefore, both of them were higher than those of the image of LKC, with better segmentation effects.

The study aimed to compare the effects of GKC and LKC on ultrasound images of 80 patients with brachial plexus block. Figure 2 shows the comparison results of Jaccard similarity ratio between two algorithms ($P < 0.05$). The results showed that the accuracy of GCK model in this study was 96.21% in platform 1 and 83.52% in platform 2. Therefore, both of them were better than those of the LKC image with better segmentation effect.

*3.2. Comparison of Basic Data of Patients from the Two Groups.* Comparison of the age, height, gender, weight, and surgical time of patients from the two groups was conducted, suggesting that the differences were not statistically obvious ($P > 0.05$). The comparison results of the average height and surgical time of patients from the two groups are shown in Figure 3.

*3.3. Ultrasound Image Characteristics of Brachial Plexus Block.* The brachial plexus nerve was divided into four areas to describe the UI characteristics, such as the level of the intermuscular groove, the level of the posterior triangle, the level of the subclavian fossa, and the level of the axilla.

The intermuscular groove was located in the space between the anterior and the middle scalene muscles. Besides, the brachial plexus nerve block of the intermuscular groove approach could block the suprascapular nerve, lateral thoracic nerve, musculocutaneous nerve, axillary nerve, and the supraclavicular branch of cervical plexus. When there was a nerve block, the sheath of the brachial plexus was a direct continuation of the dura mater, which was connected to the epidural space (Figure 4). The level of the posterior triangle of the neck was located in the supraclavicular area. In this region, the brachial plexus passes from "root" to "stem." C5 and C6 formed the upper trunk, C7 formed the middle trunk, and the lower trunk was formed by C8 and T1. The upper and middle trunks were usually located on the surface

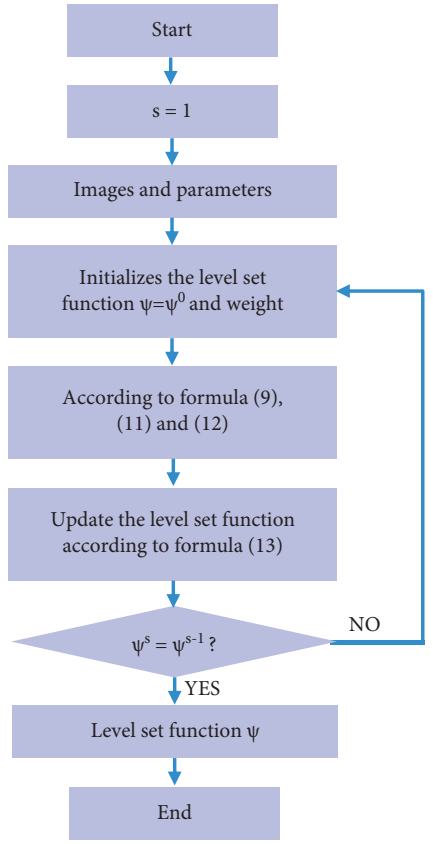


Figure 1: Flowchart of GKC.

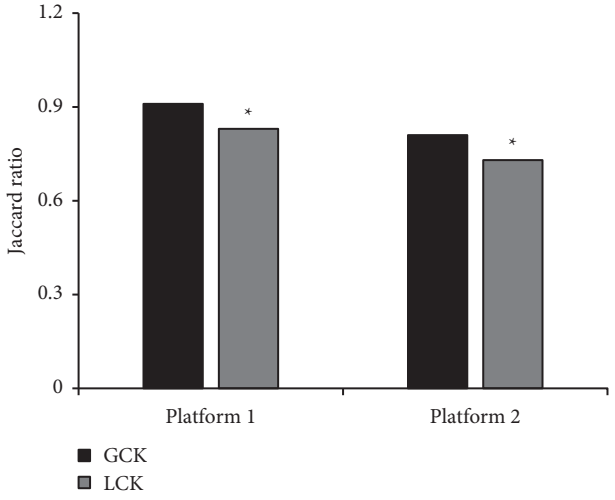


Figure 2: Comparison of Jaccard ratio between two algorithms. Note: *indicated that the comparison was statistically significant ($P < 0.05$).

or outside of the subclavian artery, while the inferior trunk was usually situated on the deep surface of the subclavian artery.

The brachial plexus block of subclavian fossa level could not block the intercostal brachial plexus but could block the brachial plexus in other areas. Thus, the brachial plexus was divided into lateral, medial, and posterior bundles at the axillary level (Figure 5). It was actually a collection of terminal nerves. The main branch of the lateral bundle was the musculocutaneous nerve, and the position of the musculocutaneous nerve had more mutations. Besides, the medial cutaneous nerves of the arm and forearm were the main branches of the medial bundle. Some small cutaneous nerve branches of the medial cutaneous nerve of the arm passed through the superficial fascia at the level of the latissimus dorsi, forming communication with the intercostal brachial nerve to innervate the skin of the inner arm. In addition, the terminal branch of the medial bundle was the ulnar nerve.

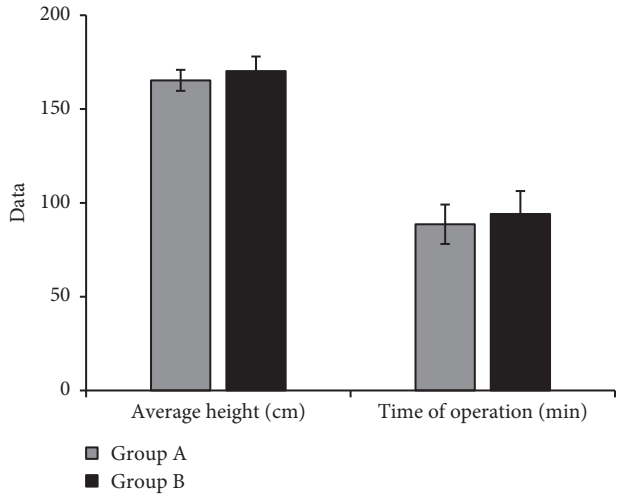


Figure 3: Comparison of the average height and surgical time of patients from the two groups.

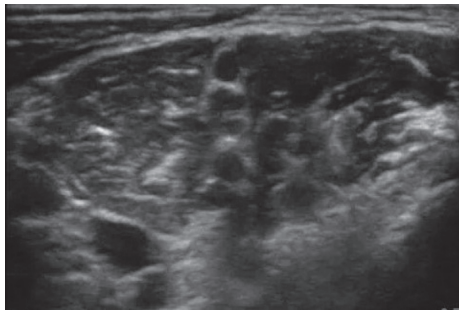

Figure 4: An image of intermuscular groove brachial plexus nerve. Note: the gap located between the anterior and the middle scalene muscles was presented in the above image. The patient was a 43-year-old male.

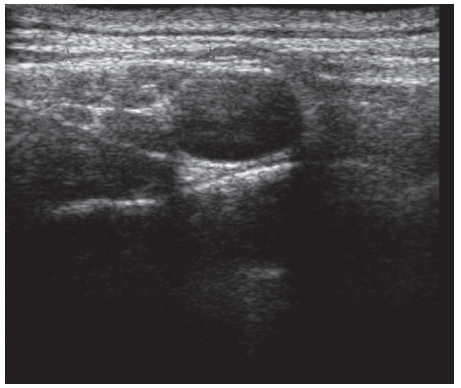

Figure 5: An image of brachial plexus block at axillary level. Note: there were visible lateral, medial, and posterior bundles. The patient was a 46-year-old male.

The main nerve branches of the posterior bundle included the radial nerve, axillary nerve, subscapular nerve, and thoracic dorsal nerve. The radial nerve usually lied behind the axillary artery and on the surface of the latissimus dorsi tendon. The axillary nerve usually accompanied the posterior circumflex artery and innervated the skin of the lower edge of the deltoid muscle. The subscapular nerve dominated the subscapularis muscle and part of the shoulder joint capsule. Furthermore, the thoracic dorsal nerve dominated the subscapular muscle and teres major.

*3.4. Surgical Progress of Patients from the Two Groups.* The time of applying tourniquet and the time of brachial plexus block of patients from the two groups were compared during the surgeries, showing that the differences were not statistically substantial within and between groups ($P > 0.05$) (Figure 6).

*3.5. Comparison of the Effects of Brachial Plexus Block in Patients from the Two Groups.* A comparison of the blocking effects of patients from both groups was conducted. The comparison results showed that the onset time of sensory block and motor block was not substantially different among patients from the two groups ($P > 0.05$) (Figure 7). The duration of sensory and motor block ($352.78 \pm 45.89$ min and $324.38 \pm 41.29$ min) in group B was significantly longer than $292.28 \pm 35.69$ min and $256.58 \pm 42.76$ min in group A, and the differences were statistically significant ($P < 0.05$) (Figure 8).

*3.6. Comparison of Different Indicators of Patients from the Two Groups.* The heart rate of patients from group A did not change greatly at different time points, and there were no obvious differences ($P > 0.05$). The heart rate of patients from group B slowed down at T1 and T2 in contrast to T0 ($P < 0.05$) (Figure 9). Figure 10 reveals that the mean arterial pressure of patients from group A at different time points had no great difference ($P > 0.05$). Compared with $84.91 \pm 8.77$ beats/min and $89.58 \pm 7.62$ beats/min in group A, the mean arterial pressure ($70.24 \pm 9.77$ beats/min and $69.89 \pm 8.97$ beats/min) in group B decreased sharply at T1 and T2 ($P < 0.05$).

*3.7. Comparison of the Postoperative Analgesia of Patients from the Two Groups.* In Figure 11, the duration of postoperative pain ($582.70 \pm 51.89$ min) in group B was longer than $372.89 \pm 49.89$ min in group A, and the difference was statistically marked ($P < 0.05$). Compared with $4.48 \pm 2.19$ in group A, postoperative pain score ($2.98 \pm 1.08$) in group B was significantly decreased ($P < 0.05$), which is shown in Figure 12. Thus, it suggested that dexmedetomidine combined local anesthetics could prolong the duration of pain and reduce the pain of patients.

## 4. Discussion

Brachial plexus block is the most generally applied method of nerve block anesthesia in clinical practice. Local anesthetics are injected around the brachial plexus nerve trunk to cause conduction block in the area controlled by the nerve. It is generally used for upper extremity surgery [10]. Dexmedetomidine has a relatively short half-life, so it can be

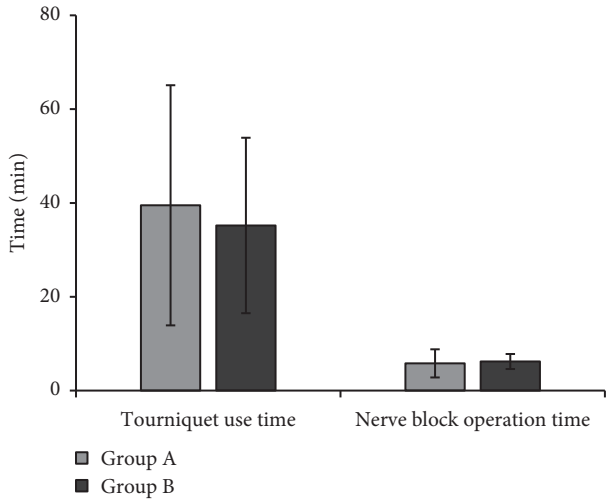


Figure 6: Indicators of patients from both groups in the surgical process.

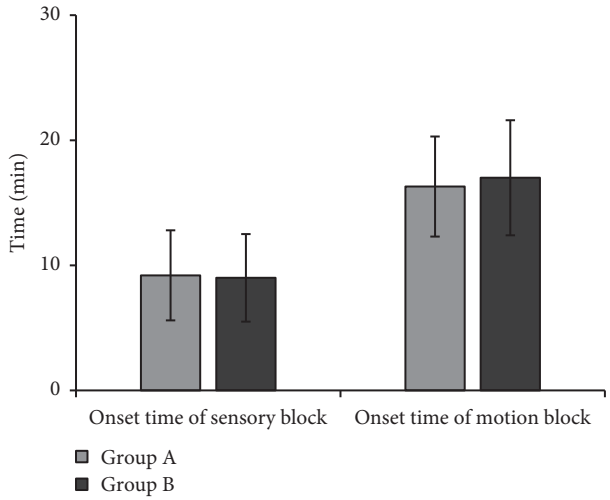


Figure 7: Comparison of the block onset time among patients from groups A and B.

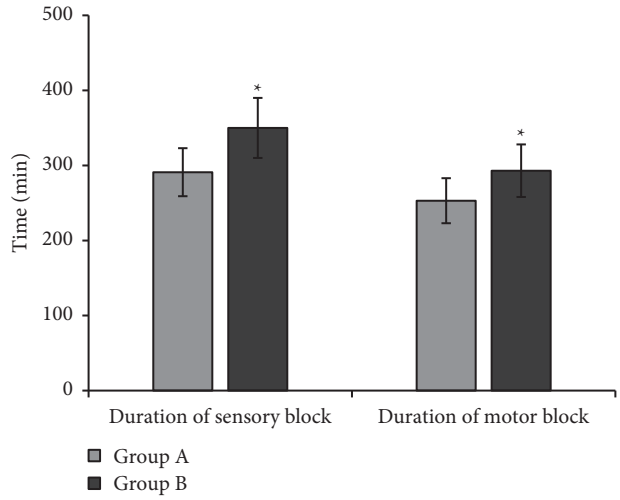


Figure 8: Comparison of the duration of block in patients from both groups. Note: *indicated that the difference was statistically remarkable in contrast to group A ($P < 0.05$).

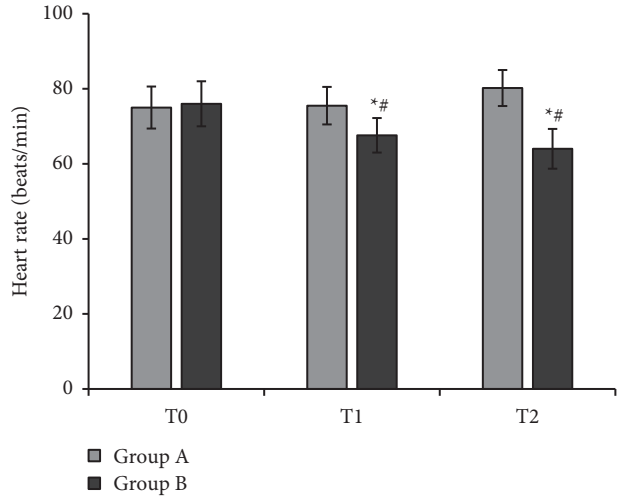


Figure 9: Comparison of the heart rates of patients from both groups at different time points. Note: * showed that the difference was statistically substantial in contrast to group B at T0 ($P < 0.05$), and # meant that there was a statistically huge difference in contrast to group A ($P < 0.05$).

used as a good intravenous anesthetic [11]. Somsunder et al. [12] adopted dexmedetomidine combined with ropivacaine to act on peripheral nerve and motor nerve block, finding that it could hugely reduce the onset time of sensory block and prolong the recovery time of peripheral and motor nerves. In this study, the duration of sensory and motor blocks was obviously prolonged, and there was no difference from the above results. Ropivacaine is an amide anesthetic, which has a longer action time, higher clearance rate, and higher safety than previous anesthetics [13], and the degree of anesthesia can be strictly controlled according to the dose of ropivacaine. Due to the above advantages, ropivacaine is extensively applied in clinical practice [14].

There was no great difference among patients from groups A and B in terms of age, height, gender, weight, and surgical time ($P > 0.05$). Besides, the duration of sensory and motor blocks in patients from group B was longer extremely than the duration of group A ($P < 0.05$). This was consistent with the research results of Jung et al. [15]. The main mechanism of action is that dexmedetomidine can indirectly drop the content of adrenaline and directly inhibit the transmission of neuronal action potential [16]. In the nerve center, dexmedetomidine can control the delivery of a certain kind of substance in the dorsal horn neuron pain pathway, so as to function as the $\alpha$-adrenergic receptor, thereby reducing the dosage of local anesthetics and decreasing the poisoning caused by local anesthetics [17].

After a certain dose of dexmedetomidine was given to patients from group A, they all showed clinical features of sleepiness and lethargy, indicating that dexmedetomidine had a sedative effect. Das et al. [18] pointed out that dexmedetomidine would slow down the heart rate and lower blood pressure. The mean arterial pressure of

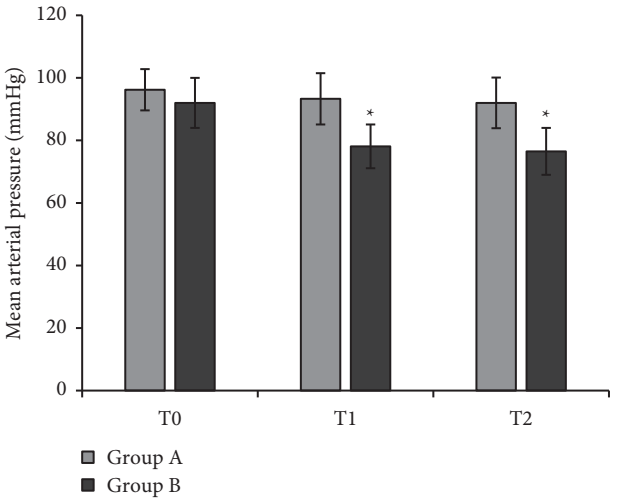


Figure 10: Comparison of the mean arterial pressure of patients from both groups at T0, T1, and T2. Note: * revealed that the difference was statistically substantial in contrast to group A ($P < 0.05$).

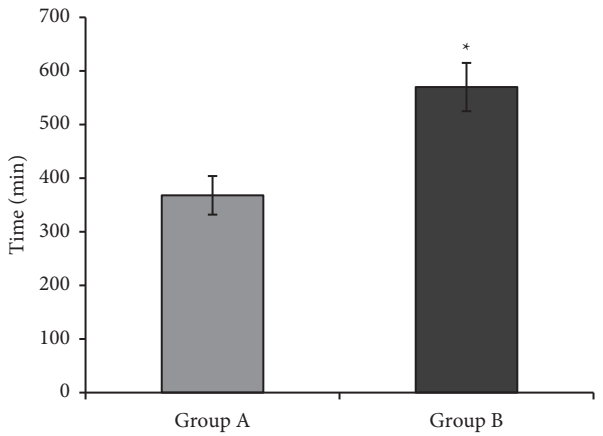


Figure 11: Comparison of the duration of first postoperative pain in patients from both groups. Note: * indicated that the difference was statistically marked in contrast to group A ($P < 0.05$).

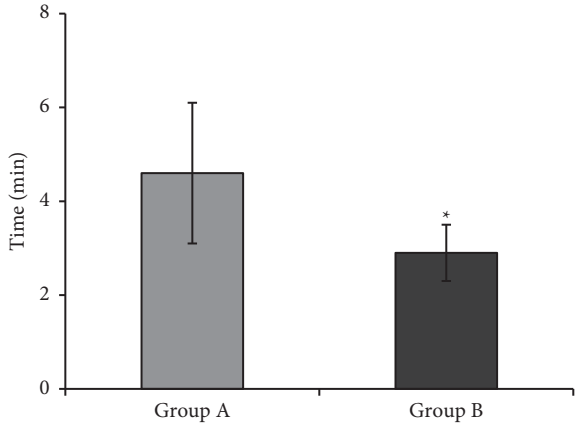


Figure 12: Comparison of the scores of first postoperative pain in patients from both groups. Note: * indicated that there was a statistically huge difference in contrast to group A ($P < 0.05$).

patients from group B in this study dropped 30 minutes after the injection of dexmedetomidine, and their heart rate slowed down. Thus, dexmedetomidine could indeed relieve anxiety in patients during surgery, reduce heart rate, and lower mean arterial pressure. The duration of first postoperative pain in patients from group B was obviously longer than the duration of group A ($P < 0.05$), suggesting that dexmedetomidine combined local anesthetics could increase the duration of pain. The first postoperative pain score of group B was dramatically lower than the score of group A ($P < 0.05$), so dexmedetomidine had an analgesic effect. The results of this study were basically consistent with initial expectations. Combined anesthesia worked better for patients. This might be related to analgesic effects of dexmedetomidine, which reduced the suggestive psychology of patients to a certain extent [19, 20].

In this study, ultrasonic images were processed by GKC and compared with LKC. The segmentation accuracy (96.21% and 83.52%) of GKC was higher than 82.21% and 70.52% of LKC ($P < 0.05$). The results indicated that no matter what platform was used, GKC algorithm had better segmentation performance. However, there was a lack of research related to this result, which lacked comparison and more conclusions to support. Therefore, it was suggested to strengthen the study of relevant experiments later.

## 5. Conclusion

The ultrasound images of 80 patients with brachial plexus block anesthesia were analyzed by GKC and LKC in turn, and it was found that the segmentation effect of GKC was superior to LKC. Dexmedetomidine combined local anesthetics could obviously enhance the effect of brachial plexus block and prolong the duration of sensory and motor nerve blocks. Dexmedetomidine had sedative and analgesic effects, so as to slow down the heart rate and lower the mean arterial pressure. However, the duration of postoperative pain was prolonged, and the degree of pain was reduced. The limitation of this study was that the health status of the subjects was good, without other comorbidities such as hypertension and diabetes. The sample size of the study was small, so the results of the study were not representative enough. Therefore, whether the results of this study were generally useful to people with comorbidities needs further study. It is suggested to expand the sample size and type in the follow-up study to make the results more convincing. To sum up, the results of this study can provide an effective method for clinical brachial plexus block surgery.

## Data Availability

The data used to support the findings of this study are available from the corresponding author upon request.

## Conflicts of Interest

The authors declare that they have no conflicts of interest.

## References


[1] C. Vandepitte, M. Kuroda, R. Witvrouw et al., "Addition of liposome bupivacaine to bupivacaine HCl versus bupivacaine HCl alone for interscalene brachial plexus block in patients having major shoulder surgery," *Regional Anesthesia and Pain Medicine*, vol. 42, no. 3, pp. 334–341, 2017.

[2] N. Hussain, V. P. Grzywacz, C. A. Ferreri et al., "Investigating the efficacy of dexmedetomidine as an adjuvant to local anesthesia in brachial plexus block," *Regional Anesthesia and Pain Medicine*, vol. 42, no. 2, pp. 184–196, 2017.

[3] C. J. Boushey, M. Spoden, F. M. Zhu, E. J. Delp, and D. A. Kerr, "New mobile methods for dietary assessment: review of image-assisted and image-based dietary assessment methods," *Proceedings of the Nutrition Society*, vol. 76, no. 3, pp. 283–294, 2017.

[4] S. Jorge, K. Pereira, H. López-Fernández et al., "Ultrasonic-assisted extraction and digestion of proteins from solid biopsies followed by peptide sequential extraction hyphenated to MALDI-based profiling holds the promise of distinguishing renal oncocytoma from chromophobe renal cell carcinoma," *Talanta*, vol. 206, Article ID 120180, 2020.

[5] K. El-Boghdadly, R. Brull, H. Sehmbi, and F. W. Abdallah, "Perineural dexmedetomidine is more effective than clonidine when added to local anesthetic for supraclavicular brachial plexus block," *Anesthesia & Analgesia*, vol. 124, no. 6, pp. 2008–2020, 2017.

[6] S. Banerjee, R. Acharya, and B. Sriramka, "Ultrasound-guided inter-scalene brachial plexus block with superficial cervical plexus block compared with general anesthesia in patients undergoing clavicular surgery: a comparative analysis," *Anesthesia: Essays and Researches*, vol. 13, no. 1, pp. 149–154, 2019.

[7] A. Abuhamad, K. K. Minton, C. B. Benson et al., "Obstetric and gynecologic ultrasound curriculum and competency assessment in residency training programs: consensus report," *Journal of Ultrasound in Medicine*, vol. 37, no. 1, pp. 19–50, 2018.

[8] S. R. Nallam, S. Chiruvella, and S. Karanam, "Supraclavicular brachial plexus block: comparison of varying doses of dexmedetomidine combined with levobupivacaine: a double-blind randomised trial," *Indian Journal of Anaesthesia*, vol. 61, no. 3, pp. 256–261, 2017.

[9] R. Kaur, M. Kaur, S. Kaur et al., "A study to compare the analgesic efficacy of dexmedetomidine and fentanyl as adjuvants to levobupivacaine in ultrasound-guided supraclavicular brachial plexus block," *Anesthesia: Essays and Researches*, vol. 12, no. 3, pp. 669–673, 2018.

[10] L. Vorobeichik, R. Brull, and F. W. Abdallah, "Evidence basis for using perineural dexmedetomidine to enhance the quality of brachial plexus nerve blocks: a systematic review and meta-analysis of randomized controlled trials," *British Journal of Anaesthesia*, vol. 118, no. 2, pp. 167–181, 2017.

[11] E. Albrecht, L. Vorobeichik, A. Jacot-Guillarmod, N. Fournier, and F. W. Abdallah, "Dexamethasone is superior to dexmedetomidine as a perineural adjunct for supraclavicular brachial plexus block," *Anesthesia & Analgesia*, vol. 128, no. 3, pp. 543–554, 2019.

[12] R. G. Somsunder, N. B. Archana, G. Shivkumar, and K. Krishna, "Comparing efficacy of perineural dexmedetomidine with intravenous dexmedetomidine as adjuvant to levobupivacaine in supraclavicular brachial plexus block," *Anesthesia: Essays and Researches*, vol. 13, no. 3, pp. 441–445, 2019.

[13] P. S. Dharmarao, R. Holyachi, and R. Holyachi, "Comparative study of the efficacy of dexmedetomidine and fentanyl as adjuvants to ropivacaine in ultrasound-guided supraclavicular brachial plexus block," *Turkish Journal of Anesthesia and Reanimation*, vol. 46, no. 3, pp. 208–213, 2018.

[14] A. Das, S. Dutta, S. Chattopadhyay et al., "Pain relief after ambulatory hand surgery: a comparison between dexmedetomidine and clonidine as adjuvant in axillary brachial plexus block: a prospective, double-blinded, randomized controlled study," *Saudi Journal of Anaesthesia*, vol. 10, no. 1, pp. 6–12, 2016.

[15] H. S. Jung, K. H. Seo, J. H. Kang, J.-Y. Jeong, Y.-S. Kim, and N.-R. Han, "Optimal dose of perineural dexmedetomidine for interscalene brachial plexus block to control postoperative pain in patients undergoing arthroscopic shoulder surgery," *Medicine*, vol. 97, no. 16, p. e0440, 2018.

[16] H. D. Rashmi and H. K. Komala, "Effect of dexmedetomidine as an adjuvant to 0.75% ropivacaine in interscalene brachial plexus block using nerve stimulator: a prospective, randomized double-blind study," *Anesthesia: Essays and Researches*, vol. 11, no. 1, pp. 134–139, 2017.

[17] V. Mangal, T. Mistry, G. Sharma, M Kazim, N Ahuja, and A Kulshrestha, "Effects of dexmedetomidine as an adjuvant to ropivacaine in ultrasound-guided supraclavicular brachial plexus Block: a prospective, randomized, double-blind study," *Journal of Anaesthesiology, Clinical Pharmacology*, vol. 34, no. 3, pp. 357–361, 2018.

[18] B. Das, M. Lakshmegowda, M. Sharma, S. Mitra, and R. Chauhan, "Supraclavicular brachial plexus block using ropivacaine alone or combined with dexmedetomidine for upper limb surgery: a prospective, randomized, double-blinded, comparative study," *Revista Espanola de Anestesiologia y Reanimacion*, vol. 63, no. 3, pp. 135–140, 2016.

[19] B. Subramaniam, P. Shankar, S. Shaefi et al., "Effect of intravenous acetaminophen vs placebo combined with propofol or dexmedetomidine on postoperative delirium among older patients following cardiac surgery," *Journal of the American Medical Association*, vol. 321, no. 7, pp. 686–696, 2019.

[20] M. Gozalo-Marcilla, F. Gasthuys, S. P. L. Luna, and S. Schauvliege, "Is there a place for dexmedetomidine in equine anaesthesia and analgesia? a systematic review (2005-2017)," *Journal of Veterinary Pharmacology and Therapeutics*, vol. 41, no. 2, pp. 205–217, 2018.